Journal of the Korean Vacuum Society
Vol. 3, No. 2, June 1994, pp. 203-206

〈연구논문〉

Growth and Characterization of $CuIn_3Se_5$ Thin Film

Chang-Dae Kim, John R. Tuttle* and Rommel Noufi*

Department of Physics, Mokpo National University, Mokpo 534-729, Korea
**National Renewable Energy Laboratory (Formerly Solar Energy Research Institute), Golden, CO 80401, USA*
(Received April 4, 1994)

$CuIn_3Se_5$ 박막의 성장과 특성

김창대 · John R. Tuttle* · Rommel Noufi*

목포대학교 자연과학대학 물리학과
*미국 *National Renewable Energy Laboratory*
(Formerly Solar Energy Research Institute)
(1994년 4월 4일 접수)

Abstract — The structural and optical properties of $CuIn_3Se_5$ thin films grown by co-evaporation have been investigated by XRD, SEM, transmission and reflectance measurements. It is confirmed from the XRD measurements that $CuIn_3Se_5$ crystallizes in a defect chalcopyrite structure with ordered Cu vacancies and an ordered exchange of Cu with In. The absorption characteristics support that the compound has a direct bandgap. The energy gap of $CuIn_3Se_5$ is found to be 1.27 eV at room temperature. The results of $CuIn_3Se_5$ thin films are discussed in comparison with those of $CuInSe_2$ thin films.

요 약 — 동시증착법으로 성장한 $CuIn_3Se_5$ 박막의 구조 및 광학적 특성을 XRD, SEM, 광투과 및 광반사 측정으로부터 조사하였다. XRD 측정에 의하면 $CuIn_3Se_5$는 정열된 Cu 빈자리와 Cu 빈자리에 In으로 대치되는 defect chalcopyrite 구조임이 확인되었다. 또한 광흡수 측정으로부터 $CuIn_3Se_5$는 금지대내에서 직접 전이에 의한 광흡수 특성을 보여주며, 이때 에너지띠 간격은 1.27 eV이었다. $CuIn_3Se_5$ 박막에 대한 연구결과들은 $CuInSe_2$의 결과들과 비교하여 논의하였다.

1. INTRODUCTION

$CuInSe_2$ has attracted considerable attention because it is a promising material for high-efficiency photovoltaic devices due to its desirable band gap ($E_g \simeq 1.0$ eV) and relatively high absorption coefficient ($\alpha = 10^4 \sim 10^5\ cm^{-1}$) [1]. Recently a conversion efficiency of up to 14.8% has been achieved in $CuInSe_2$-based solar cells [2]. For further optimization of solar cell design, a better understanding of various phases in the Cu-rich and In-rich composition as well as $CuInSe_2$ is necessary. A number of single phase compounds, i.e., $CuIn_2Se_{3.5}$ [3-5], $Cu_3In_5Se_9$ [6-8], $CuIn_3Se_5$ [5, 9-11], Cu_5InSe_4 [5, 12] and $CuIn_5Se_8$ [13] have been reported in the Cu_2Se-In_2Se_3 pseudo-binary phase studies. Among them the compound $CuIn_3Se_5$ appears to be one of the most important heterojunction partner of $CuInSe_2$ because of the perfect matching of the lattice between two materials [14]. However, a systematic investigation on the physical properties of $CuIn_3Se_5$ has not been made up to date. In view of a literature survey [15] of the compound, there exists the discrepancy concerning its structure and

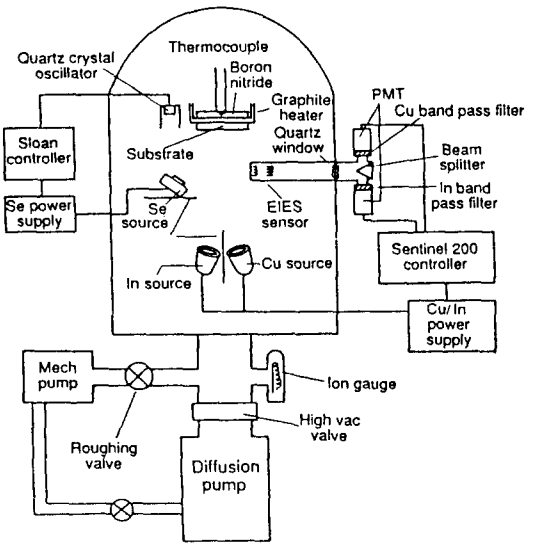

Fig. 1. Vacuum thin film co-evaporation system.

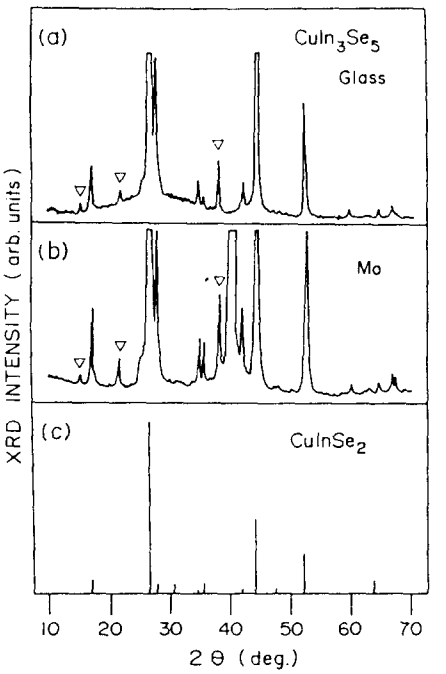

Fig. 2. XRD patterns of $CuIn_3Se_5$ thin films grown on bare and Mo-coated glass and $CuInSe_2$ thin films grown on bare glass.

homogeneity range.

In this paper we report the structural and optical properties of $CuIn_3Se_5$ thin films using X-ray diffraction (XRD), scanning electron microscopy (SEM), optical transmission and reflection measurements. The results are also discussed in comparison with $CuInSe_2$.

$CuIn_3Se_5$ and $CuInSe_2$ thin films were prepared by vacuum thermal evaporation of the constituent elements onto heated 1 in. ×2 in. substrates of bare and Mo-coated glass using the co-evaporation system of Fig. 1. The Cu and In arrival rates are monitored and controlled to within 0.05 Å/s by a Sentinel 200 deposition control system utilizing electron impact emission spectroscopy (EIES) as the detection mechanism for feedback to the source power supplies. The Se flux and Cu/In calibrations are accomplished with a quartz crystal monitoring(QCM) technology. Actual substrate surface temperature of 500 ℃ was assured by calibration. Two film thicknesses of the same composition were obtained from a single run by shielding half of the substrate during the deposition. The film thickness ranged from 0.5 μm for optical measurements to 1.0 μm for structural characterization. Film thickness determination is accomplished by a Tencor Profilometer with auto-leveling features. XRD measurements were made with Rigaku DMAX vertical goniometer and controller system with a rotating Cu-anode X-ray generator and tungsten filament. Composition determination was accomplished by EPMA and the composition of the films grown was measured to be Cu=10.38 at%, In=33.97 at% and Se=55.65 at%, i.e., slightly In-rich and Se-rich relative to the composition 1:3:5.

Optical measurements are performed with a 5240 Beckman spectrophotometer in the wavelength range 800~2000 nm, with an integrating sphere to measure diffuse and total reflectance, R_{diff} & R_{tot}, and scattered and total transmission, T_{scatt} & T_{tot}. Reflectance measurements are normalized to the absolute reflectance of a $BaSO_4$ plate.

Fig. 2 shows the XRD patterns of $CuIn_3Se_5$ films grown on bare and Mo-coated glass in comparison with those of $CuInSe_2$. In the XRD patterns of $CuIn_3Se_5$ films the only differences between the two substrates, other than the Mo peak ($2\theta=40.50$), is a possible orientation for the films grown on bare and Mo-coated glass. Comparing the XRD patterns

Table 1. XRD data of $CuIn_3Se_5$ and CuInSe

hkl	$CuInSe_2$			$CuIn_3Se_5$			$\Delta(2\theta)$
	2θ	d(Å)	I/I_o	2θ	d(Å)	I/I_o	
002	--	--	--	15.35	5.768	2	--
101	17.12	5.179	5	17.25	5.136	5	+.13
110	--	--	--	21.90	4.005	3	--
112	26.64	3.343	100	26.89	3.313	100	+.25
103	27.72	3.216	3	27.99	3.185	10	+.27
004	30.77	2.903	<1	--	--	--	--
200	30.89	2.892	<1	--	--	--	--
202	34.62	2.589	≪1	34.95	2.565	3	+.33
211	35.53	2.525	3	35.81	2.505	3	+.28
114	--	--	--	38.35	2.345	5	--
105	41.88	2.155	1	42.30	2.135	4	+.42
213	41.97	2.151	1	〃	〃	〃	+.33
204	44.16	2.049	44	44.56	2.032	62	+.40
220	44.26	2.045	22	〃	〃	〃	+.30
301	47.78	1.902	1	--	--	--	--
116	52.24	1.750	12	52.80	1.732	11	+.56
312	52.40	1.745	24	〃	〃	〃	+.40
215	52.94	1.728	≪1	--	--	--	--
224	54.87	1.672	≪1	--	--	--	--
321	57.99	1.589	≪1	--	--	--	--
314	59.70	1.548	≪1	60.29	1.534	1	+.59
008	64.09	1.452	3	64.79	1.438	1	+.70
400	64.38	1.446	6	〃	〃	〃	+.41
402	66.59	1.403	≪1	67.15	1.393	2	+.56

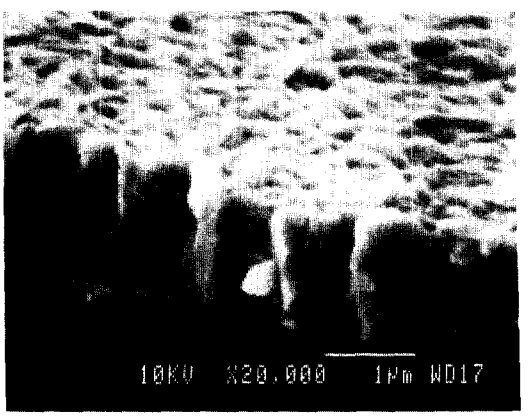

Fig. 3. SEM X-sectional micrographs of $CuIn_3Se_5$ thin films grown on bare glass.

of $CuIn_3Se_5$ with those of $CuInSe_2$, the XRD patterns of $CuIn_3Se_5$ are very similar to those of $CuInSe_2$ with the chalcopyrite structure and only three additional peaks with weak peaks at $2\theta = 15.35$, 21.90 and 38.35 are observed. These are compatible with

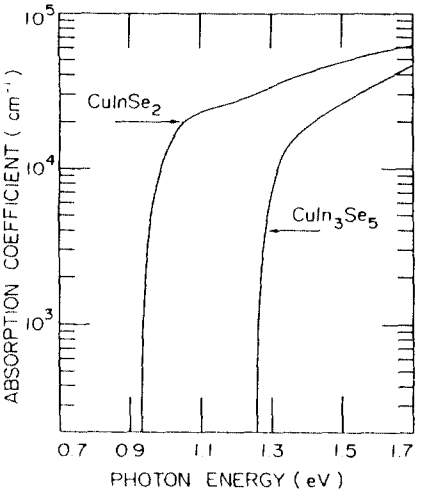

Fig. 4. Absorption coefficient α vs incident photon energy for two thin films of $CuIn_3Se_5$ and $CuInSe_2$.

(002), (110) and (114) lattice planes of $CuIn_2Se_{3.5}$ [4, 16], respectively. The occurence of the additional peaks is explained by ordered Cu vacancies and an ordered exchange of Cu with In [16]. Thus it is belived that $CuIn_3Se_5$ crystallizes in a defect chalcopyrite structure. The lattice constants of $CuIn_3Se_5$, obtained from the XRD data, are found to be $a = 5.764$ Å and $c = 11.528$ Å without any obserable tetragonal distortion, but which are slightly smaller than $a = 5.780$ Å and $c = 11.614$ Å of $CuInSe_2$. In Table 1, the XRD data are summarized for both $CuIn_3Se_5$ and $CuInSe_2$. The shifts in d-spacings (2θ) due to the lattice shrinkage are observed in $CuIn_3Se_5$. Such shifts are also observed when the composition is changed from Cu-rich to In-rich and the substrate temperature is varied from 350℃ to 500℃ in $CuInSe_2$ [16]. In Fig. 3 SEM X-sectional morphology of thin film $CuIn_3Se_5$ is shown. The grain size for the films is about 1.0 μm and the film roughness is smooth.

Fig. 4 depicts the optical absorption coefficient, α, as a function of the photon energy $h\nu$, of $CuIn_3Se_5$ thin films. It was calculated from the measurements of diffuse and total reflection, R_{diff} & R_{tot}, and scattered and total transmission, T_{scatt} & T_{tot}. As can be seen in Fig. 4, the magnitude of the absorption coefficient above the fundamental band edge of the $CuIn_3Se_5$ films is about $10^4\ cm^{-1}$, which is slightly

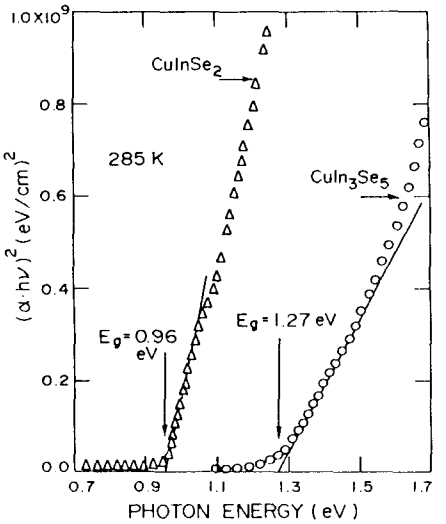

Fig. 5. Plots of $(\alpha \cdot h\nu)^2$ vs photon energy for two thin films of $CuIn_3Se_5$ and $CuInSe_2$.

smaller than that of the $CuInSe_2$ films. It is also observed that there is a decrease in α with In concentration for In-rich $CuInSe_2$ [17]. The absorption edge, even in this high α regime, is observed to be quite abrupt for the $CuIn_3Se_5$ as well as for the $CuInSe_2$ with a direct band gap. The fundamental absorption, which manifests itself by a rapid rise in absorption, can be used to determine the energy gap of the compounds.

In allowed direct transitions the absorption coefficient is given by

$$\alpha \cdot h\nu = A(h\nu - E_g)^{1/2} \quad (1)$$

where A is a constant and E_g is the energy gap. Therefore, for a direct band gap semiconductor, the $(\alpha \cdot h\nu)^2$ vs $h\nu$ characteristics is predicted to be a straight line, with a photonenergy axis intercept indicative of the band gap. This is illustrated in Fig. 5. Extrapolation of $(\alpha \cdot h\nu)^2 = 0$ in Fig. 5 indicates the direct band gap of 1.27 eV for the $CuIn_3Se_5$ films and 0.96 eV for the $CuInSe_2$ films, respectively.

In summary, thin films of $CuIn_3Se_5$ and $CuInSe_2$ have been grown by co-evaporation and the structural and optical properties of these films have been determined. The compound $CuIn_3Se_5$ crystallizes in a defect chalcopyrite structure with ordered Cu vacancies and an ordered exchange of Cu with In. The absorption characteristics confirm that $CuIn_3Se_5$ has a direct band gap. The energy gap deduced from these measurements is about 1.27 eV for $CuIn_3Se_5$ films and 0.96 eV for $CuInSe_2$ films.

Acknowledgment

This work was supported by the KOSEF of the Republic of Korea.

References

1. A. Rockett and R. W. Birkmire, *J. Appl. Phys.* **70**, R81 (1991).
2. L. Stolt, J. Hedström, J. Kessler, M. Ruckh, K. O. Velthaus and H. W. Schock, *Appl. Phys. Lett.* **62**, 597 (1993).
3. C. Djega-Mariadassou, R. Lesueur, J. Leloup and J. H. Albany, *Phys. Lett.* **65A**, 455 (1978).
4. B. Schumann, G. Kühn, U. Boehnke and H. Neels, *Sov. Phys. Crystallogr.* **26**, 678 (1981).
5. M. L. Fearheiley, *Solar Cells* **16**, 91 (1986).
6. V. I. Tagirov, N. F. Gakhramanov, A. G. Guseinov, F. M. Aliv and G. G. Guseinov, *Sov. Phys. Crystallogr.* **25**, 237 (1980).
7. V. I. Tagirov, N. F. Gakhramanov, A. G. Guseinov and F. M. Alivg, *Sov.Phys. Semicond.* **14**, 831 (1980).
8. N. M. Gasanly, A. G. Guseinov, E. A. Aslanovand and S. A. El-Hamid, *Phys. Stat. Sol. (b)* **158**, K85 (1990).
9. D. M. Ganbarov, G. G. Guseinov and Z. Sh. Karaev, *Neorg. Mater.* **8**, 2211 (1972).
10. W. Hönle, G. Kühn and U.-C. Boehnke, Cryst. Res. Technol. **23**, 1347 (1988).
11. J. Kessler, D. Schmid, R. Schäffler, H. W. Schock and S. Menezes, Proc. the 23rd IEEE. Photovoltaic Specialists Conference, Louisville (IEEE, New York, 1993), p. 549.
12. K. J. Bachmann, M. L. Fearheiley, Y. H. Shing and N. Tran, *J. Appl. Phys. Lett.* **44**, 407 (1984).
13. C. Manolikas, J. V. Landuyt, R. D. Ridder and S. Amelinckx, *Phys. Stat. Sol. (a)* **55**, 709 (1979).
14. D. Schmid, M. Ruckh, F. Grunwald and H. W. Schock, *J. Appl. Phys.* **73**, 2902 (1993).
15. U.-C. Boehnke and G. Köhn, *J. Mat. Sci.* **22**, 1635 (1987).
16. J. R. Tuttle, Ph.D. Dissertation (Univ. Colorado, 1990).
17. J. R. Tuttle, D. Albin, R. J. Matson and R. Noufi, *J. Appl. Phys.* **66**, 4408 (1989).